Numerical Evaluation of an Add-On Vehicle Protection System

Geneviève Toussaint, Amal Bouamoul, Robert Durocher, Jacob Bélanger*, Benoît St-Jean

Defence Research and Development Canada – Valcartier
2459 Bravoure Road, Quebec (Qc), G3J 1X5, Canada

*Numerica Technologies Inc.

1 Introduction

Defence Research and Development Canada (DRDC) has been involved in programs to reduce the vulnerability of vehicles to mines and improvised explosive devices for many years. In this work, DRDC was mandated to design and optimize an add-on vehicle protection system. Testing an entire vehicle against improvised explosive devices or blast landmines is both time-consuming and expensive; therefore, to reduce costs, numerical simulations using the LS-DYNA® hydrocode [1] were performed to support the development phase of the protection system. A finite element model of a simplified full-scale model of the vehicle called a mock-up was developed for this purpose. This model included the critical sections that were likely to be affected by a threat. Finite element studies were then performed to compare the performance of several protection designs and to orient on the choice of the final one.

This paper presents the loading model that was used to simulate the effect of a landmine on the structure, the finite element (FE) models of the baseline and of three concepts and finally, a comparison of the relative performance of the different protection system designs.

2 Loading model

Several approaches have been used to simulate the loading profile generated by landmines [2]. Studies such as in [3 to 6], presented the mine impulse loading model developed at DRDC, which transforms the specific impulses given by Westine's empirical equation [7] into initial velocities that can be applied as initial conditions to nodes of shell elements located in the direct line of sight from the mine to the structure. The empirical equation of Westine *et al.* [7] that predicts the specific impulse imparted to a flat plate placed over a buried landmine is provided below [3]:

$$i_v(x,y) = 0.1352\left(1+\frac{7\delta}{9z}\right)\left(\frac{\tanh(0.9589\zeta d)}{\zeta d}\right)^{3.25}\sqrt{\frac{\rho E}{z}} \tag{1}$$

$$\zeta = \frac{\delta}{z^{\frac{5}{4}} A^{\frac{3}{8}} \tanh\left(\left(2.2\frac{\delta}{z}\right)^{\frac{3}{2}}\right)} \tag{2}$$

where z is the stand-off distance of plate P (parallel to the ground) to the center of the mine, E is the energy release by the explosive charge, ρ is the density of soil, δ is the burial depth to the center of the mine and A is the cross-sectional area of the mine, $d=\sqrt{(x^2+y^2)}$ is the radial distance from the center of the mine. Four criteria, depending on δ, z, E, A, d, ρ and the seismic P-wave velocity in the soil, must be met when using equation 1 [3].

One limitation of this impulse model is its inability to load a FE structure made of solid elements. Therefore, a pressure-based mine loading model was developed by DRDC to address this limitation. This model, mainly based on the Westine impulse model [3, 7], uses a pressure time-space distribution to apply the loading conditions on the structure. To validate this model, a series of numerical simulations were conducted with various pressure time-space distribution functions and different coefficients and the results were compared with experimental data. The general form of the pressure *P(t)* calculated on a solid element is shown in Figure 1:

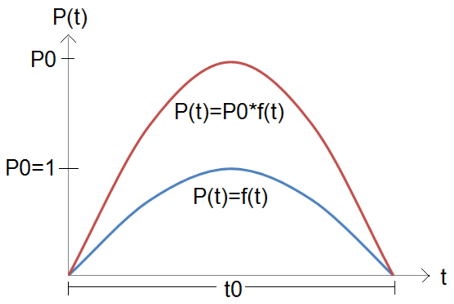

Fig. 1: Pressure as a function of time

$$P(t) = P_0 f(t) \tag{3}$$

where P_0 is the maximum pressure applied on a solid element and it is determined using the specific impulse (I_s) predicted by Westine.

$$P_0 = I_s \int f(t) \tag{4}$$

where *f(t)* is a user input function and is defined as:

$$f(t) = \left(1 - \frac{t}{t_0}\right) e^{\left(-a\frac{t}{t_0}\right)} \sin(\beta t) \tag{5}$$

where t is the current time, t_0 is a user input constant and corresponds to the time for which the pressure is applied (after t_0, the loading is equal to 0), $\beta = \pi * t / t_0$ and a is a constant.

This model has the flexibility to apply initial conditions on solid elements that are mainly in the direct line of sight from the mine. Parameters such as mine characteristics (i.e. diameter, mass, explosive nature), the location and depth of burial are considered and can be modified depending on the conditions to be simulated.

3 Numerical simulations

3.1 Finite element models

The FEMAP software [8] was used to generate and mesh the simplified full-scale model of the baseline mock-up, as shown in Figure 2.

Each part of the CAD model was meshed with Lagrangian solid elements using a constant stress solid element formulation and for shell elements with Belytschko-Tsay formulation and 2 integration points in the thickness. The FE model contained approximately 65 000 elements. The *mat_plastic_kinematic* model implemented in LS-DYNA [1] was used to model the material response for each part of the mock-up. The plate was 5083-H321 Aluminium [9] while brackets were defined by ASTM A572 Steel, grade 50 properties [9]. Additional lumped masses were distributed over several strategic locations on the model to represent the additional mass of the vehicle. Gravity loading was applied to all parts of the model.

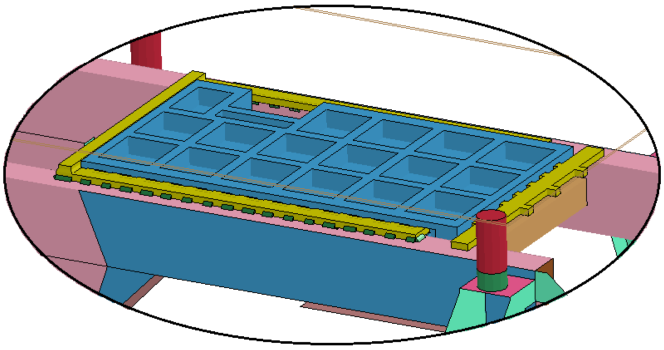

Fig. 2: General view of the mock-up

A *contact_automatic_single_surface* and *contact_automatic_surface_to_surface* keywords were used to define the contacts between all parts. The pressure based mine loading model was used to apply the initial loading genereted by a landmine detonation under the structure.

Table 1: Material properties [9]

		5083-H321	**ASTM A572 G50**	**ASTM A514**
Density, ρ	kg/m^3	2660	7850	7850
Young's modulus, E	GPa	70.3	205	205
Poisson's ratio, ν		0.33	0.29	0.29
Yield stress, σ_y	MPa	200	345	690
Tangent modulus	MPa	726	504	396

To meet a higher level of protection, modifications to the baseline add-on protection system had to be investigated. Numerical simulations were thus performed during the development phase on several concepts to help design and optimize a new mine-protection system that can be used to protect a specific vehicle. Figure 3 shows close-up and exploded views of the baseline protection system as well as for three concepts. In general, all protection systems were composed of a plate (in blue), welds (in green) and brackets (in yellow).

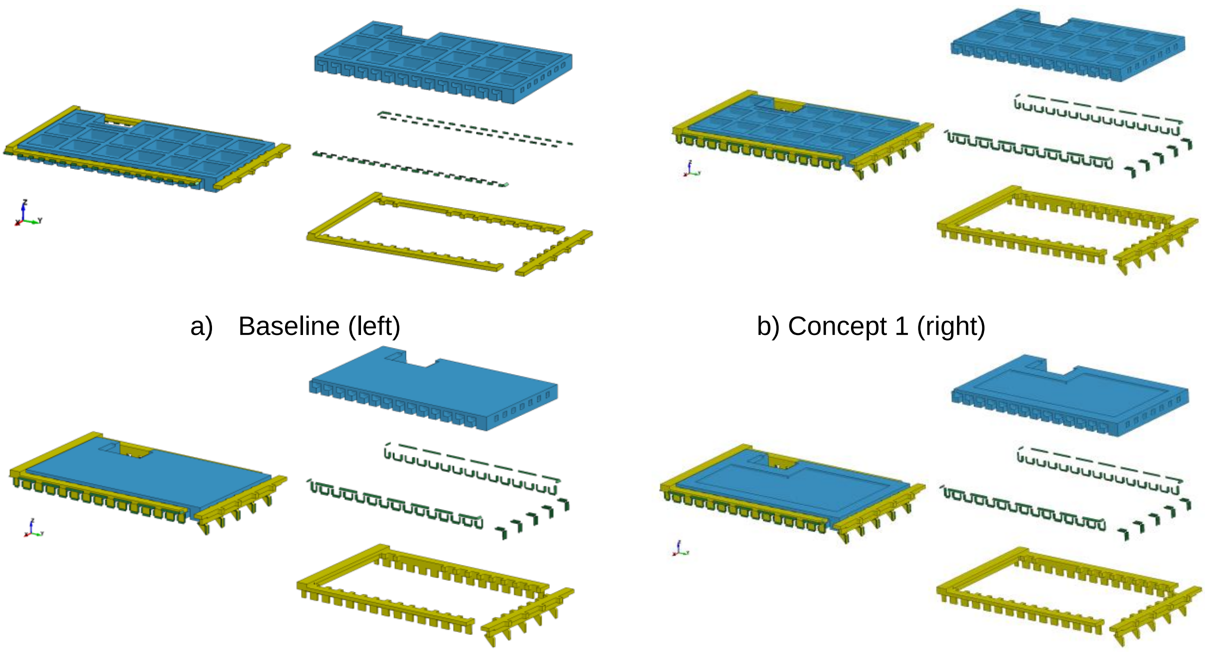

a) Baseline (left)

b) Concept 1 (right)

c) Concept 2 (left)

d) Concept 3 (right)

Fig. 3: Protection systems

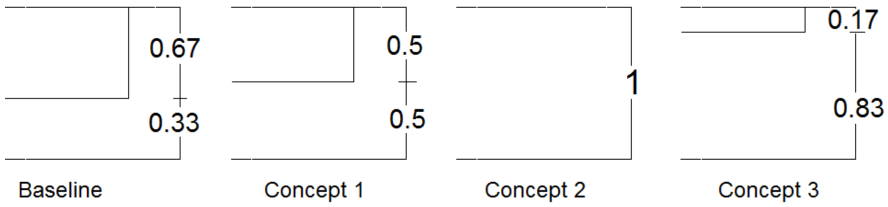

Fig. 4: Comparison of the relative thicknesses of the protection plate a) Baseline (waffle cross-section) b) Concept 1 (waffle cross-section) c) Concept 2 (full plate) d) Concept 3

Figure 4 presents a comparison of a cross-section of view of the protection plate for each concept. The maximum thickness of each concept had the same value and was scaled to one. The main difference between the baseline and Concept 1 was an increase in the waffle plate thickness by 17% (see Figures 4a and b respectively). In addition, welds and brackets were both strictly modified to increase the attachments rigidity. The second and third concepts are shown in Figures 3c and 3d, respectively. The design of the welds and brackets of Concept 2 were the same as in Concept 1 except that the brackets material was replaced for ASTM A514 steel [9] and the material used to define the welds was changed. Concept 2 was also modeled with a full plate. For Concept 3, the only difference with Concept 2 is that some material was removed from the entire middle section of the plate to increase the distance between the plate and the floor and therefore, allow for more deflection of the plate below the floor while reducing slightly the mass of the protection system. Figure 5 shows a comparison of the mass of the protection systems relative to the baseline protection system. The mass of the protection system over the entire mass of the vehicle corresponds to 0.88%, 1.11%, 1.45% and 1.35% for the baseline, Concepts 1, 2 and and 3 respectively.

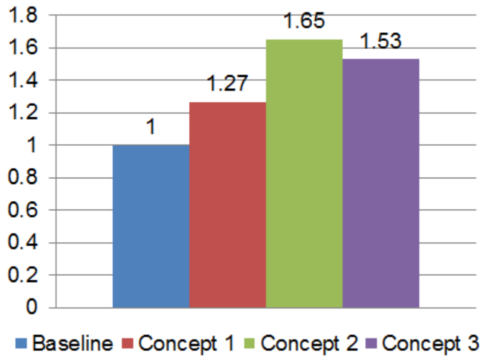

Fig. 5: Comparison of the relative mass of the protection systems

3.2 Comparison

The following section presents a comparison of the displacement and deformation of the four configurations. Figure 6 shows a higher displacement of the plate for the baseline and Concept 1 as compared to Concepts 2 and 3. Figure 7 demonstrates clearly that the deformation of the baseline and Concept 1 is much larger than in the case of Concepts 2 and 3.

Figures 8 and 9 present the normalized Von-Mises stresses in the protection plate for the baseline and Concept 3.

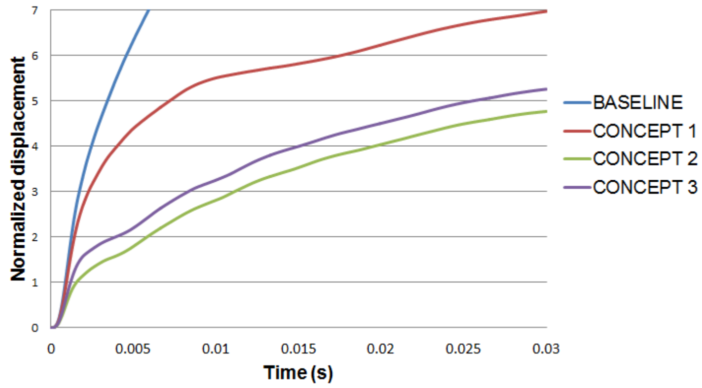

Fig. 6: Normalized displacement

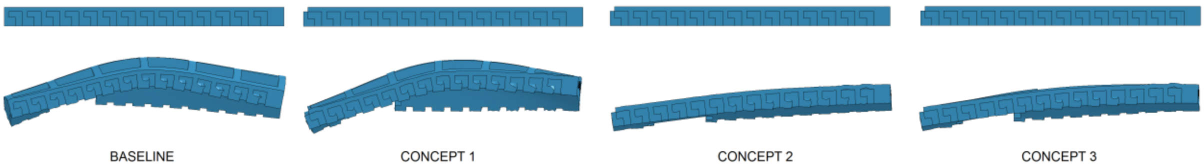

Fig. 7: Deformation of the plate.

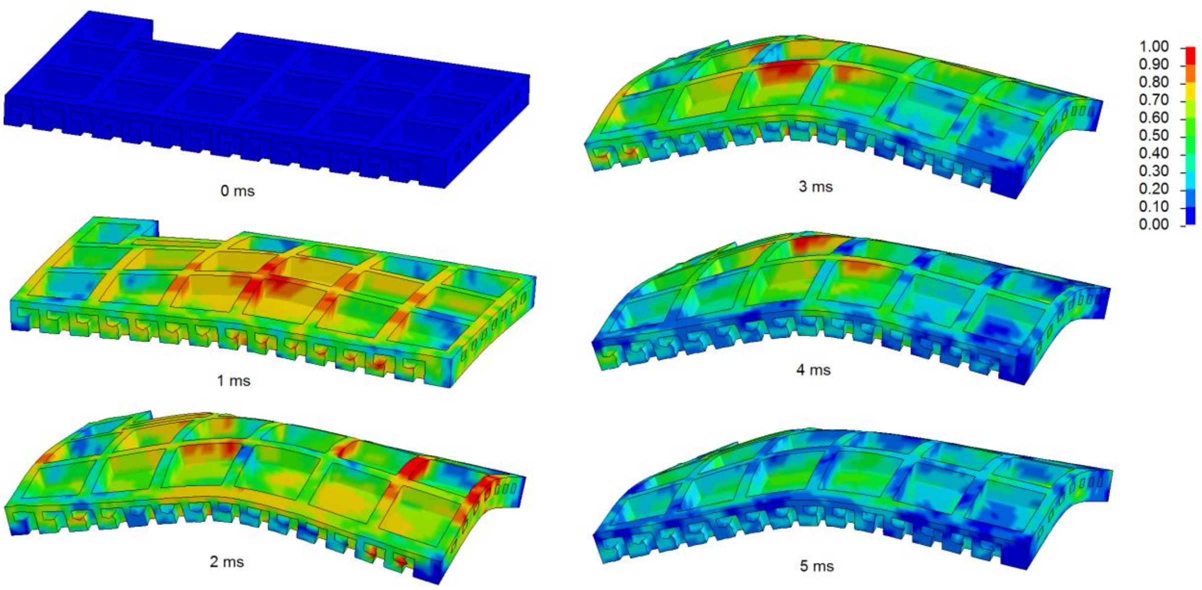

Fig. 8: Normalized Von-Mises stresses (Baseline)

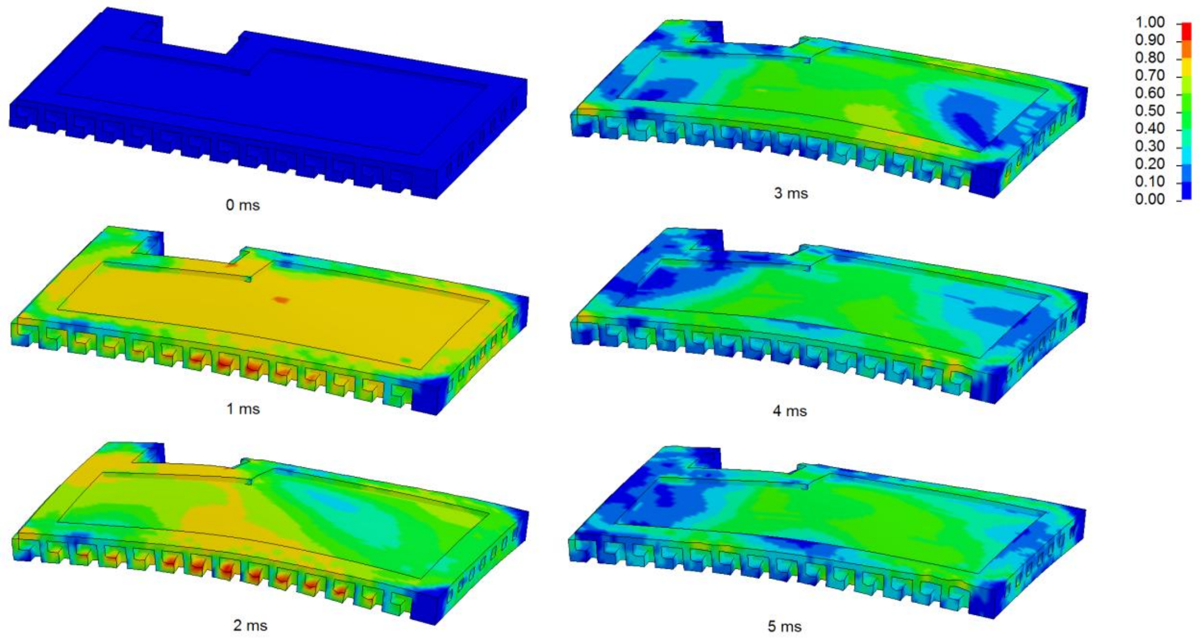

Fig. 9: Normalized Von-Mises stresses (Concept 3)

Figure 10 shows a comparison of the strains in the brackets and in the welds between the baseline and Concept 3. The baseline showed high strains in almost all the attachment points while in Concept 3 there was fewer strains localised in only few attachment points.

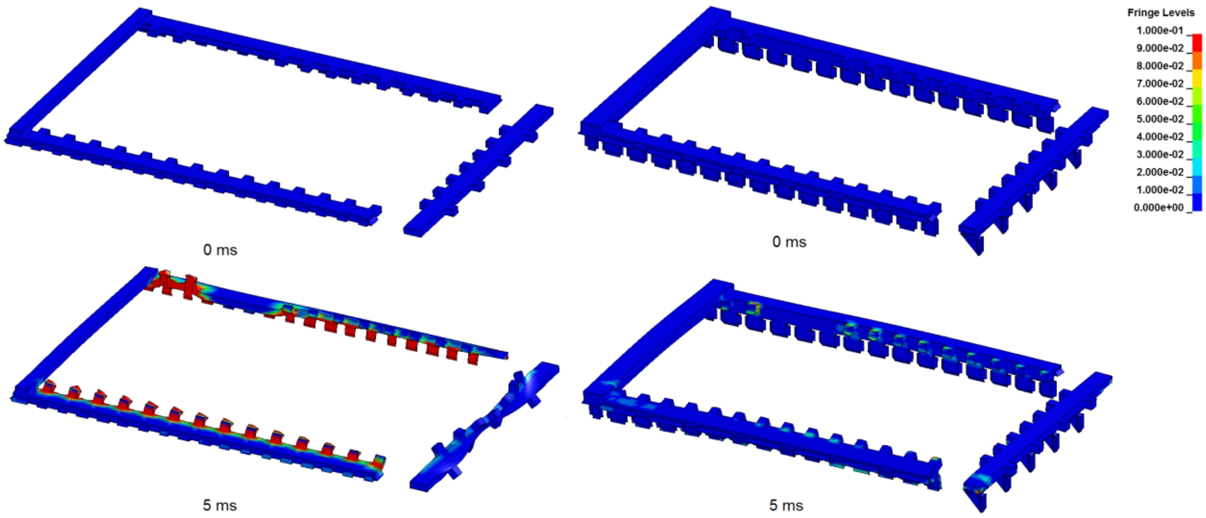

a) *Baseline (left)* b) *Concept 3 (right)*

Fig. 10: Effective Plastic Strain

Based on the finite element analyses, the modifications incorporated into Concepts 2 and 3 showed an improvement in the performance compared to the baseline performance in terms of deformation of the plate and the rigidity of the attachments to the frame. Concepts 2 and 3 are the concepts that absorb most of the energy from the mine and deforme less compared to the other configurations. Concepts 2 and 3 show better energy absorption capacity than the other configurations.

4 Summary

In this study, finite element simulations were performed during the development phase of a modified protection system of a vehicle, to compare the performance of several concepts. Concepts 2 and 3 showed an increase performance when compared to the other designs from an energy absorption standpoint.

The combination of numerical simulations and a progressive experimental test program proved to be an efficient approach to evaluate concepts, to perform option analyses and to design a successful mine-protection system. The approach of using a combination of a progressive experimental program in conjunction with numerical analysis methods help to refine the numerical models to provide improved accuracy and increase the confidence of the predictive capability of the numerical analyses. Finite element simulations contributed considerably to reduce the costs and time in developing and choosing the best concept.

The modeling of welds was not fully investigated and is the subject of future work.

5 Acknowledgments

The authors would like to thank Dr. Claude Fortier, Mr. Stéphane Dumas and Mr. Jean-Luc Bédard for their input to this work.

6 References

[1] Livermore Software Technology Corporation, www.lstc.com.
[2] Toussaint G. and Bouamoul A. *Comparison of ALE and SPH methods for simulating mine blast effects on structures*. DRDC Valcartier. TR 2010-326. Unclassified. Unlimited distribution. (2010).
[3] Tremblay J. *Impulse on Blast Deflectors from a Landmine Explosion*. DRDC Valcartier. DREV-TM-9814. Unclassified. Unlimited distribution. (1998).
[4] Williams K. and Poon K. *A Numerical Analysis of the Effect of Surrogate Anti-Tank Mine Blasts on the M113*. DRDC Valcartier. DREV TM-2000-007. Unclassified. Unlimited distribution. (2000).
[5] Williams K., McClennan S., Durocher R., St-Jean B. and Tremblay J. *Validation of a Loading Model for Simulating Blast Mine Effects on Armoured Vehicles*, 7th International LS-DYNA Users Conference. (2002).
[6] Williams K. and Fillion-Gourdeau F. *Numerical Simulation of Light armoured Vehicle Occupant Vulnerability to Anti-Vehicle Mine Blast*, 7th International LS-DYNA Users Conference. (2002).
[7] Westine P. S., Morris B. L., Cox P.A. and Polch E.Z. *Development of Computer Program For Floor Plate Response From Land Mine Explosions,* Southwest Research Institute. (1985).
[8] www.plm.automation.siemens.com/en_us/products/velocity/femap/index.shtml
[9] www.matweb.com